Fuel Processing Technology 200 (2020) 106310

Contents lists available at ScienceDirect

Fuel Processing Technology

journal homepage: www.elsevier.com/locate/fuproc

Research article

Chemisorption and physisorption of fine particulate matters on the floating beads during Zhundong coal combustion

Jing Zhao[a,b], Yufeng Zhang[a,b], Xiaolin Wei[a,b,*], Teng Li[a], Yu Qiao[c]

[a] State Key Laboratory of High-Temperature Gas Dynamics, Institute of Mechanics, Chinese Academy of Sciences, Beijing 100190, China
[b] School of Engineering Science, University of Chinese Academy of Sciences, Beijing 100049, China
[c] State Key Laboratory of Coal Combustion, Huazhong University of Science and Technology, Wuhan 430074, China

ARTICLE INFO

Keywords:
Floating beads
Fine particulate matter
Pulverized coal combustion
Mineral elements
Chemisorption
Physisorption

ABSTRACT

Floating beads rich in silica-aluminum oxide are hollow glass microspheres that can be obtained from fly ash by flotation. Floating beads have the advantages of high yield, low cost and easy access in the power plants or industrial kilns and are used as the sorbent for reducing the fine particulate matter (PM) emissions during pulverized coal combustion in this work. The pulverized coals mixed with floating beads are burned in an electrically heated drop-tube furnace at 1573 K. The size distribution and yield of PM are analyzed by an electrical low pressure impactor (LPI). The results indicate that the internal mineral elements, especially Na/K, Ca, and S, form a large amount of PM during pulverized coal combustion and floating beads can efficiently reduce PM formation via chemisorption and physisorption. With floating beads addition, the yield of ultrafine mode particles ($PM_{0.5}$), mainly consisted of Na/K and S, decreases by 55.76%, and the yield of central mode particles ($PM_{0.5-7}$), mainly consisted of Ca, Fe and Si, decreases by 21.7%. The surface reaction (chemisorption) between mineral vapors and sorbent particles reduces the $PM_{0.5}$ emissions, and $PM_{0.5+}$ can be reduced by the particles colliding and coalescing (physisorption), resulting in aluminosilicates on the surface of the sorbents. The results gained from characterization tests show that floating beads have more active sites and free silicon dioxides due to the broken Si—O and Al—O bonds after high-temperature calcination, thereby promoting the capture of mineral vapors such as alkali metals.

1. Introduction

Zhundong coal, which is produced in Xinjiang District, China, plays a dominant role in energy resources [1–3]. However, the combustion of Zhundong coal with high contents of alkali and alkaline earth metals (AAEMs) will not only promote slagging and corrosion on the high-temperature surface of heat exchangers [4–7] but also cause fine particulate matter (PM) emissions [8–12]. PM, especially $PM_{2.5}$, is one of the main sources of haze, and $PM_{2.5}$ has aerodynamic particles with diameters less than 2.5 μm [10,13]. Usually, fine PM contains a large amount of toxic and harmful substances and seriously threatens the environment and human health due to its long-term residence in the atmosphere [8,14,15]. Although the electrostatic precipitators (ESPs) and bag filters installed in coal-fired power plants can efficiently capture most ash particles [16–18], a significant portion of fine PM escapes to the atmosphere due to its high penetration into the control devices [16–19]. Therefore, to promote the clean and efficient use of Zhundong coal, power plants must take effective measures to reduce fine PM emissions. Among them, the combustion of coal mixed with sorbents is considered a promising approach to further reduce the formation of fine PM in the furnace [10,20,21].

Previous studies [22–24] have proven that aluminosilicate-based sorbents, such as kaolin, can efficiently capture metal vapors through complex physical and chemical processes during coal combustion. Takuwa [25] and Sun et al. [10] reported that kaolin could adsorb mineral vapors, such as alkali metals, through surface reactions and thereby inhibit the formation of ultrafine particles. The main products were regarded as aluminosilicates, e.g., sodium aluminosilicate (Na-Al-Si). Si and Liu et al. [8] found that Na-Al-Si had a lower deformation temperature and could melt and form a softening layer on the surface of sorbents. The reduction in central mode particles ($PM_{0.5-2.5}$) was closely associated with the collision and coalescence of particles and Na-Al-Si [26]. Similar findings have also been confirmed by the studies of Ninomiya [27] and Wang et al. [28], who thought Mg-based sorbent could react with minerals to form aluminosilicates such as Mg-Al-Si. The coalescence of fine PM can be enhanced due to liquid formation.

* Corresponding author at: State Key Laboratory of High-Temperature Gas Dynamics, Institute of Mechanics, Chinese Academy of Sciences, Beijing 100190, China.
E-mail address: xlwei@imech.ac.cn (X. Wei).

https://doi.org/10.1016/j.fuproc.2019.106310
Received 30 August 2019; Received in revised form 18 November 2019; Accepted 4 December 2019
Available online 13 December 2019
0378-3820/

However, kaolin is a kind of mineral products, has become the papermaking, ceramics, rubber, chemical industry, coating, medicine and national defense and other dozens of industries necessary mineral raw materials. In China, it is only distributed in a few provinces and resources are very scarce. Moreover, with the strengthening of ecological protection in China, the exploitation of kaolin, as a scarce resource, has been controlled, so the application of kaolin is limited in actual power plants. Therefore, it is necessary to develop more types of sorbents to meet the needs of the coal-fired power plants. According to the special physical and chemical characteristics, kaolin provides much guidance and reference for searching new sorbent.

In this paper, we investigate the chemisorption and physisorption of fine particulate matters on the floating beads during Zhundong coal combustion. The production of floating beads is very huge in China. Floating beads are not only from power plants, but also from fly ash of various industrial kilns. Floating beads are hollow glass microspheres that can be obtained from fly ash by flotation and are usually used as heat-insulating materials because of their low thermal conductivity and high melting point [29]. However, up to now, no reports about the use of floating beads as sorbents for reducing fine PM. Unlike the traditional Si- Al sorbents such as kaolin, in terms of physical shape, the shape of floating beads is more regular after calcination at high temperature and the voidage between particles is larger. In addition, floating beads have a larger external surface area due to a lower density. Therefore, the mineral vapors such as alkali metals are more likely to diffuse to the surface of the floating beads during reaction. In terms of chemical composition, floating beads are mainly composed of silicon-aluminum oxides (approximately 60% SiO_2 and 35% Al_2O_3) Compared to kaolin (approximately 50% SiO_2 and 45% Al_2O_3), floating beads have higher percent of SiO_2. Some studies [10,21] have proven that the formation of free silicon dioxide at high temperatures will facilitate the adsorption of fine PM. Therefore, in addition to the higher percentage of SiO_2, it can be inferred that the floating beads may contain more free silicon dioxide than do the conventional Si-Al sorbents due to high-temperature calcination in the furnace. In addition, Sun, et al. [10] reported that kaolin needed to be pretreated before it could show a good adsorption effect. Therefore, considering the equipment and transportation cost, the total price of floating beads is basically cheaper than that of kaolin in China. The adsorption of mineral vapors such as alkali metals by floating beads will have more practical significance. So, do floating beads have the excellent physical and chemical properties on reducing fine PM emission? If so, how does it work? These issues need to be clarified.

To evaluate the adsorption characteristics fine PM on the floating beads during coal combustion, in this paper, kaolin and kaolin (T) are selected as a reference. Three types of sorbents that had been mixed physically with Zhundong pulverized coal were burned in a lab-scale electrically heated drop-tube furnace (DTF). First, the influence of minerals in coal on fine PM formation is investigated by comparing the yield of $PM_{0.5}$ and $PM_{0.5+}$ between the combustion processes of raw coal and leached coal. Second, the PM adsorption capability of floating beads and kaolin is compared by an analysis of the collected ash particles. Finally, based on the experimental results, composition analysis of fine PM, and the characterizations of sorbents, the function mechanisms of sorbents on controlling the yield of PM are revealed during coal combustion. At the same time, the different adsorption methods and paths of Si-Al sorbents on ultrafine mode particles and central or coarse mode particles are summarized.

2. Experimental section

2.1. Experimental materials

A Chinese coal named Zhundong coal is selected as the experimental coal sample. The sample is pulverized and sieved to particle sizes between 40 and 100 μm. The results of ICP-OES show that Na in Zhundong coal is mainly presented in the form of water-soluble, ammonium acetate and acid-soluble with mass fraction of 78.42%, 11.57%, and 6.44%, respectively. And the remaining 3.57% is the insoluble-Na in the form of aluminosilicate. Na is usually released as NaCl and NaOH, and the stable Na_2SO_4 can be produced in the presence of SO_2, H_2O, and O_2. The three types of alkali metals are the main precursor of fine PM. Therefore, Zhundong coal rich in high content of alkali metals makes it suitable for determining the ability to capture fine PM by the Si-Al sorbents [11,30]. The detailed properties of the sieved coal are presented in Table 1.

Table 1
Ultimate and proximate analyses of tested coals.

Proximate analysis (w_{ad} %)				Ultimate analysis (w_{ad} %)					
M	A	V	FC	C	H	O	N	S	Cl
14.1	10.08	26.22	49.6	58.36	2.12	13.59	0.41	1.34	0.11

Ash analyses of tested coals									
SiO_2	Al_2O_3	Fe_2O_3	CaO	MgO	TiO_2	SO_3	P_2O_5	K_2O	Na_2O
16.61	5.86	15.33	22.66	3.94	0.44	29.18	0.24	0.58	3.10

The Si-Al sorbents, i.e., floating beads, kaolin, and kaolin (T), are used as the additives for the coal combustion experiments. Before the experiments, the additives are physically mixed with raw coal at a mass ratio of 5 g-sorbents/100 g-coal. To prevent the effect on PM_{10} generation, the sorbents are sieved to particle sizes between 45 and 75 μm, and the detailed compositions of sieved samples are presented in Table 2.

2.2. Coal combustion and PM sampling

The goal was to explore the characteristics of sorbent adsorption of fine PM during Zhundong coal combustion. The PM reduction ratio of the raw coal samples, with and without additives, is analyzed and calculated via coal combustion experiments in an electrically heated DTF. As shown in Fig. 1, the DTF consists of a feed system, an electric heating furnace, a control cabinet, and a gas distributor [13,20]. The feeder is a disc vibrating micro-powder that continuously feeds coal into the furnace at a set rate (0.26 g/min for coal/coal blend samples). Pulverized coal is burned in the corundum reaction tube inside the furnace body, the length of the reaction zone is 1440 mm, and the inner diameter is 40 mm. The reaction temperature is controlled at 1573 K. The reaction atmosphere is 21% vol O_2 balanced with 79% vol N_2 during the combustion experiments, and the flow rate of simulated air is 8 L/min. The simulated air is sent to the feeder to be mixed with the pulverized coal, and then the pulverized coal is carried into the reaction tube. The pulverized coal is always nearly burned out under the given reaction conditions.

In Fig. 1, the PM generated during combustion is sampled and collected after quenching by N_2-gas (flow rate: 2 L/min) in a sampling probe (the temperature of the top point of the sampling probe is approximately 773 K), and the sampling system mainly contains a

Table 2
Composition analysis of floating beads, kaolin, and kaolin (T).

Samples	Composition (%)							
	SiO_2	Al_2O_3	Na_2O	K_2O	CaO	MgO	Fe_2O_3	SO_3
Floating beads	61.81	33.6	0.62	0.93	0.22	0.86	0.44	0.17
Kaolin	51.84	45.73	0.69	0.67	0.09	0.69	0.23	1.8
Kaolin (T)[a]	53.75	43.81	0.34	0.55	0.11	0.73	0.22	0

[a] Thermal-treated kaolin in the muffle furnace at 1273 K.

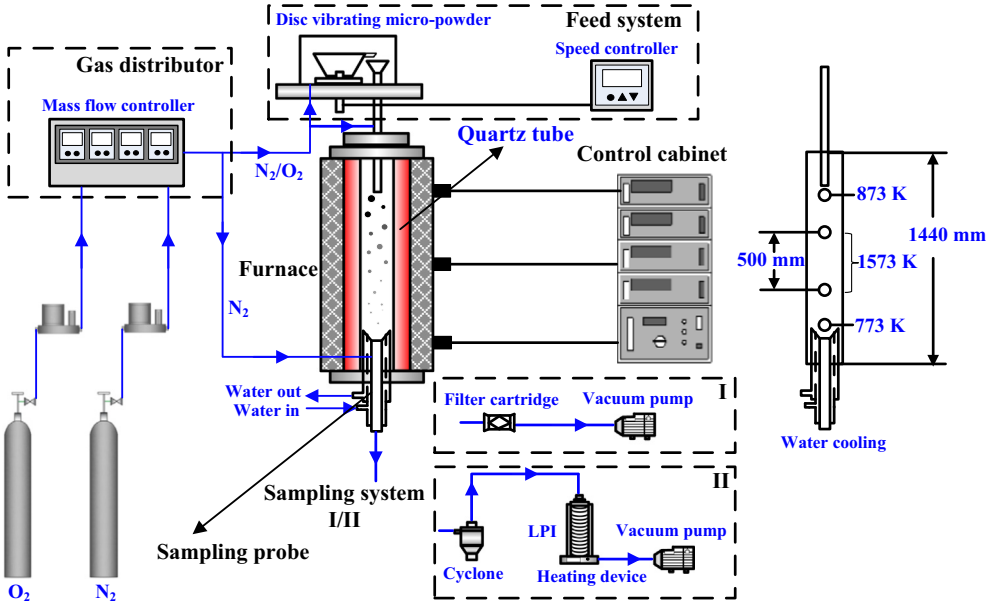

Fig. 1. Schematic diagram of the experimental setup-drop tube furnace with a quartz reactor.

cyclone, Dekati low-pressure impactor (LPI) or filter cartridge [18,20], heating device, pressure gauge, and vacuum pump. The cyclone removes the coarse particles with aerodynamic diameters larger than 10 μm, and the particles smaller than 10 μm are further separated into 14 stages based on particle size. Aluminum foil covered with Apiezon-L resin is used as the substrate for PM_{10} collection in each stage of the LPI, and the mass particle size distribution and composition of the particles are obtained [11]. The cyclone separator, the LPI, and the connecting pipe are heated and kept at 403 K to avoid the condensation deposition of SO_x and H_2O gaseous products in the flue gas during the operation of the system. The time is set at approximately 3 min to prevent particles from bouncing off the substrates due to the long sampling time. Each PM sampling experiment is repeated at least three times to ensure satisfactory reproducibility and accuracy.

2.3. Sample analysis

The mass of PM collected in each stage of the LPI is obtained by a precision electronic balance (Sartorius M2P, accuracy: 1 μg), and the difference before and after the sampling experiments can be used as the mass of the corresponding stage of the PM. The fine PM in the size range of 7–10 μm is referred to as PM_{7-10}, representing the coarse mode particles; those in the size range of 0.5–7 μm are termed $PM_{0.5-7}$, representing the central mode particles; and those with a size less than 0.5 μm are called $PM_{0.5}$, representing the ultrafine mode particles. The concentrations of elements in the PM of each stage are determined by scanning electron microscopy (JSM-7800F, JEOL, Japan) with an energy dispersive spectrometer (SEM-EDS).

The composition analysis of sorbents is analyzed by XRF using an energy dispersive instrument (E3, Netherlands). The surface characteristics of three Si-Al sorbents are also obtained through SEM-EDS. Crystalline phase and inorganic structure analysis are determined by X-ray diffraction (XRD) using a Rigaku D/MAC/max 2500 V/PC instrument (DX2700, China) with Cu Kα radiation (40 kV, 200 mA, and λ = 1.5148 Å). The diffractometer data of XRD are acquired at a step size of 0.02° for 2θ values from 5° to 80°. To characterize the difference in the structure among the three Si-Al sorbents, the additives are analyzed by a Fourier transform infrared (FTIR) spectrometer (Bruker Tensor 27 spectrometer, Germany) in the regions of 4000–400 cm^{-1} recorded using the potassium bromide (KBr) pellet technique. In addition, to further analyze the characteristics of sorbent adsorption, the specific surface area of the sorbent samples is provided by a surface area analyzer (ASAP 2020).

3. Results and discussion

3.1. Effect of minerals in coal on PM emissions

Before discussing the experimental results regarding the PM captured by sorbents, the effect of minerals in coal on the PM emissions is first analyzed. Vaporization-condensation of mineral elements (Na, Cl, S, etc.) is the main reason for $PM_{0.5}$ formation. The dominant mechanisms are considered homogeneous nucleation because of the high concentration of metallic vapors [18,24]. $PM_{0.5+}$ emission is mainly caused by char fragmentation, coarse mineral fragmentation, and aggregation of fine molten particles [22,31,32]. Fig. 2 illustrates the $PM_{0.5}$ and $PM_{0.5+}$ emissions during the combustion of raw coal and leached coal. The raw coal after mineral leaching can be defined as leached coal [8], which can be obtained through the following steps: the coal samples are sequentially extracted with deionized water, 1 mol/L ammonium acetate (NH_4OAc), and 1 mol/L hydrochloric acid (HCl), respectively, and then repeatedly flushed with deionized water and dried at 333 K. As shown in Fig. 2, compared to the raw coal, the yield of $PM_{0.5}$ significantly decreased from 1.256 to 0.462 mg/g-coal during leached

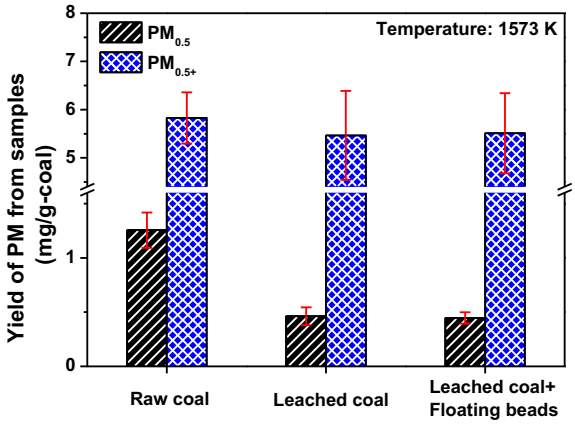

Fig. 2. Effect of mineral compounds on PM formation.

coal combustion. As a result of the sequential extraction, most of the active minerals (Na, Cl, S) in coal are leached out. This result indicates that minerals are the main elements for $PM_{0.5}$ formation. Therefore, the reduced release of mineral elements will help inhibit the generation of ultrafine particles during coal combustion. Most studies identify that Si-Al sorbents, e.g., kaolin, reduce ultrafine mode particles due to the efficient capture of mineral elements [18,25–27]. The main product of the surface reaction between sorbents and mineral vapors is considered to be aluminosilicates, e.g., Na-Al-Si (T). In addition, leached coal shows no considerable effect on $PM_{0.5+}$ emissions if the error bars are considered in Fig. 2. Minerals have a dual effect on $PM_{0.5+}$ formation. Except for vaporing into the flue gas, some leached minerals, e.g., NaCl and Na_2SO_4, may interact with minerals in the coal to form eutectics, which exacerbates the mineral coalescence and inhibits $PM_{0.5+}$ emissions. However, the organically bound sodium also exhibits a good catalytic effect on the reaction of carbon with gaseous media [33], which can induce a more intense fragmentation of chars and promote $PM_{0.5+}$ formation.

Fig. 2 also shows that the addition of floating beads has no influence on $PM_{0.5}$ and $PM_{0.5+}$ during leached coal combustion, indicating that floating beads are unlikely to interact with coal/char particles during combustion. The only plausible reason is the interaction between floating beads and minerals released from coal/char combustion, which reduces PM. $PM_{0.5}$ can be directly absorbed via the reaction between floating beads and minerals to form aluminosilicates, e.g., Na-Al-Si (T). The aluminosilicates have a lower deformation temperature and can melt and form a softening layer on the surface of sorbents. Due to aluminosilicate formation, $PM_{0.5+}$ reduction can be attributed to the collision and melting coalescence between fine PM and softening sorbent particles to form larger particles. Local turbulence in the furnace can be formed through char fragmentation and the disturbance of larger particles to the flow field, and the inertial impaction will play a vital role in $PM_{0.5+}$ particles colliding with the softening layer, resulting in the capture of $PM_{0.5+}$ by the sticky surface of the sorbent particles. The detailed analysis of the PM captured by floating beads will be further discussed in the next section.

3.2. Mass-particle size distributions and yields of ash particles collected from PM

The mass size distributions of raw coal and coal with sorbents during combustion are presented in Fig. 3. The x-axis represents the aerodynamic diameter of PM, and the y-axis represents the yields of PM and is scaled by “mg/g-coal”. Kaolin is considered to be an effective sorbent by several studies on PM reduction. Kaolin and kaolin (T) are selected as a reference to evaluate the PM adsorption characteristics on

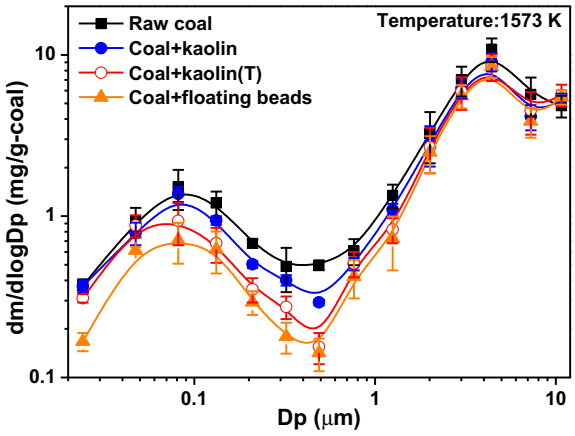

Fig. 3. Mass-based particle size distribution of PM_{10} with different Si-Al sorbent additions.

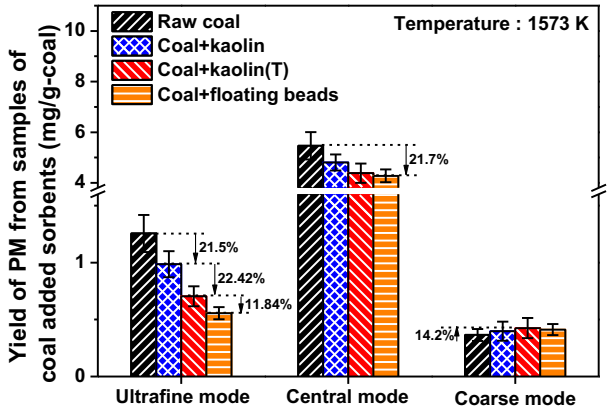

Fig. 4. Comparison of PM emissions with and without sorbents during coal combustion in O_2/N_2 atmosphere.

the floating beads. All four curves present a bimodal distribution with the peak of the ultrafine model ($PM_{0.5}$) at approximately 0.1 μm and the peak of the central model ($PM_{0.5–7}$) at approximately 4 μm. PM values larger than 7 μm in diameter are defined as coarse mode. As illustrated in Fig. 3, kaolin and floating beads can significantly decrease the concentration of ultrafine mode and central mode PM. The unique physical and chemical properties cause them to have a relatively good performance in terms of PM reduction, especially regarding the high content of silicon/aluminum. The worst adsorption characteristic of raw kaolin is mainly due to some of its defects, such as small specific surface area and low chemical reactivity. After high-temperature calcination, its physical and chemical properties are improved; thus, kaolin (T) shows a better effect in terms of PM reduction [10]. Floating beads are also a kind of Si-Al adsorbent after high-temperature calcination and exhibit the best adsorption ability among the three sorbents. As shown in Table 2, this result may be due to its higher content of active silica, which promotes PM adsorption.

The yield of PM from coal with and without sorbent combustion can be seen in Fig. 4. There is an obvious mass decrease in the ultrafine mode ($PM_{0.5}$) and central mode ($PM_{0.5–7}$), which indicates that both kaolin and floating beads have the ability to reduce the fine PM emissions, especially for the ultrafine mode. With the addition of raw kaolin, the yield of $PM_{0.5}$ decreases from 1.256 to 0.986 mg/g-coal, corresponding to a reduction efficiency of 21.5%. Compared to the case with the addition of raw kaolin, the total mass yield of $PM_{0.5}$ further decreases by 22.42% with the addition of kaolin (T). Floating beads have the highest reduction ratio, and the total mass yield of $PM_{0.5}$ decreases by 55.76%. Although the mass yield of the central mode also decreases obviously from 5.465 to 4.227 mg/g-coal, corresponding to a reduction efficiency of 21.7%, the adsorption effect of the floating beads on the central mode particles is much lower than that of the ultrafine mode. The same phenomenon is also observed for the cases with the addition of kaolin and kaolin (T). In addition, the mass yield of the coarse mode increases slightly, indicating that the addition of sorbents promotes the process of agglomeration and nucleation from fine PM to coarse PM. The above results indicate that as with kaolin, floating beads can also achieve good PM reduction efficiency, especially for the ultrafine mode ($PM_{0.5}$). According to the analysis in the previous section, the silicon-aluminum oxide in the floating beads can capture the minerals, e.g., alkali metals, efficiently by surface chemical reaction; thus, this method can significantly reduce the formation of ultrafine particles. The resulting aluminosilicates, e.g., Na-Al-Si (T), have a lower softening temperature [34] and are capable of forming a softening layer on the surface of the PM, thereby capturing the central mode particles by particle collisions.

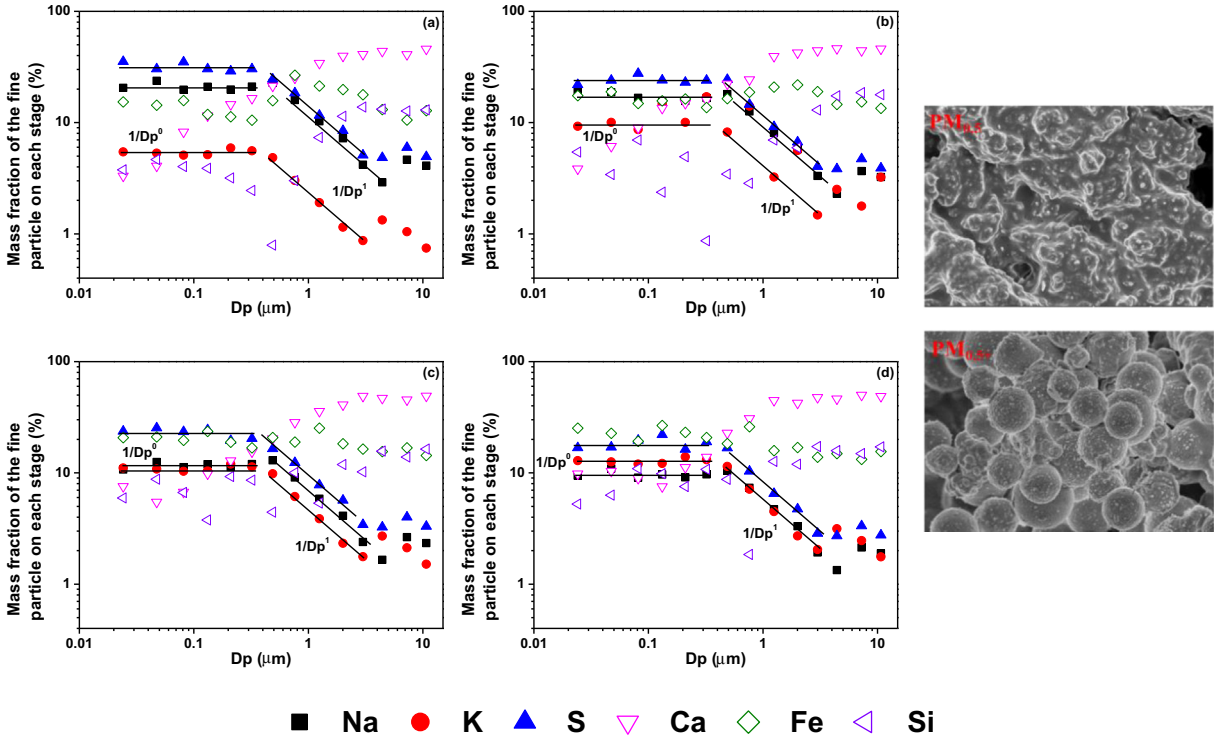

Fig. 5. Mass fraction of Na, K and S as a function of aerodynamic diameter during combustion: (a) raw coal; (b) coal + kaolin; (c) coal + kaolin (T); (d) coal + floating beads.

3.3. Composition analysis of PM generated from coal combustion

To further illustrate the fine PM formation mechanisms and the reason for the PM reduction with the addition of sorbents during Zhundong coal combustion, the compositions of PM are drawn in the form of particle size distributions, as shown in Fig. 5(a). The $PM_{0.5}$ from Zhundong coal combustion mainly consists of Na, K, S, and Fe, and the main components of $PM_{0.5+}$ are Ca, Si, and Fe. The presence of sulfur in $PM_{0.5}$ is mainly caused by the reaction of SO_2 with intermediate products, e.g., alkali metals, and the resulting sulfate condenses once the temperature is lower than the dew point [22]. The gasification rate of iron is intermediate, and there is no significant change in the content of particles of different particle sizes [11]. Fig. 5(a) shows that the concentrations of Na, K, and S in the particles less than 0.5 μm in size remain constant over the Dp, indicating that the homogeneous nucleation/condensation controls the enrichment of Na, K, and S in the ultrafine particles. With increasing particle size, the mass fractions of Na, K, and S obviously decrease. The contents of Na, K, and S in the particles with diameters in the range of 0.5–4 μm show a 1 / Dp size dependence, indicating that the surface reaction of Na, K, and S vapors with ash or sorbent particles controls the deposition on these particles [18,35]. Hence, floating beads and kaolin additions are useful for capturing Na, K, and S to reduce ultrafine mode particles. The char and coarse mineral fragmentation controls the formation of central and coarse mode particles; thus, the mass fractions of Ca and Si are relatively high in $PM_{0.5+}$ due to the lower gasification ratios of Na and K. This result further indicates that the sorbents are unlikely to capture $PM_{0.5+}$ directly by chemical reaction to reduce its concentration. During Zhundong coal combustion, the softening layer formation on the particle surface by the aluminosilicates can promote the adsorption of the central mode particles by collision to form larger particles, which is the main way to reduce $PM_{0.5+}$.

As shown in Fig. 5(b), the mass fraction of Na and S in $PM_{0.5}$ is decreased with kaolin addition, indicating that kaolin can capture the mineral vapors such as alkali metals. This will inhibit the formation of sulfate and reduce its homogeneous nucleation/condensation to form ultrafine particulate matters. The same phenomenon can be also found in Fig. 5(c) and (d), and the mass fraction of Na and S is further reduced with kaolin (T) or floating beads addition, indicating that kaolin (T) and floating beads have a more significant adsorption effect on the mineral vapors such as alkali metals, especially for floating beads. For example, with 5% floating beads addition, the mass fraction of Na in $PM_{0.5}$ is decreased from about 20% to 10%, and the mass fraction of S decreased from about 30% to 12%. This conclusion is consistent with the results gained from Figs. 3 and 4, which indicates that floating beads addition can significantly inhibit Na and S to form the ultrafine particulate matters.

3.4. Function mechanism of sorbents on controlling the yield of PM during combustion

According to the above experimental results, floating beads and kaolin can significantly control PM emissions and are bound up with the chemical reaction between sorbents and mineral vapors, e.g., alkali metals. Compared to kaolin and kaolin (T), floating beads exhibit better control of PM formation during Zhundong coal combustion. To evaluate the physical and chemical characteristics of floating beads and kaolin, a series of characterization tests are carried out to analyze the differences.

SEM images of the surface of kaolin and kaolin (T) are shown in Fig. 6(a) and (b), respectively, and the surfaces are rough, and the particles appear as dotted or polygonal blocks. After high-temperature calcination, the internal pores of kaolin (T) increase, and the specific surface area also improves due to dihydroxylation, as shown in Table 3. The BET surface area of kaolin (T) improves from 4.24 of raw kaolin to 4.53 m^2/g, corresponding to an increase of approximately 12%. In addition, kaolin (T) has more active sites and a higher reactivity to capture alkali metal vapors due to the generation of derived metakaolin [10]. Therefore, the kaolin (T) modified by calcination can better reduce the formation of fine particles due to changes in the physical and

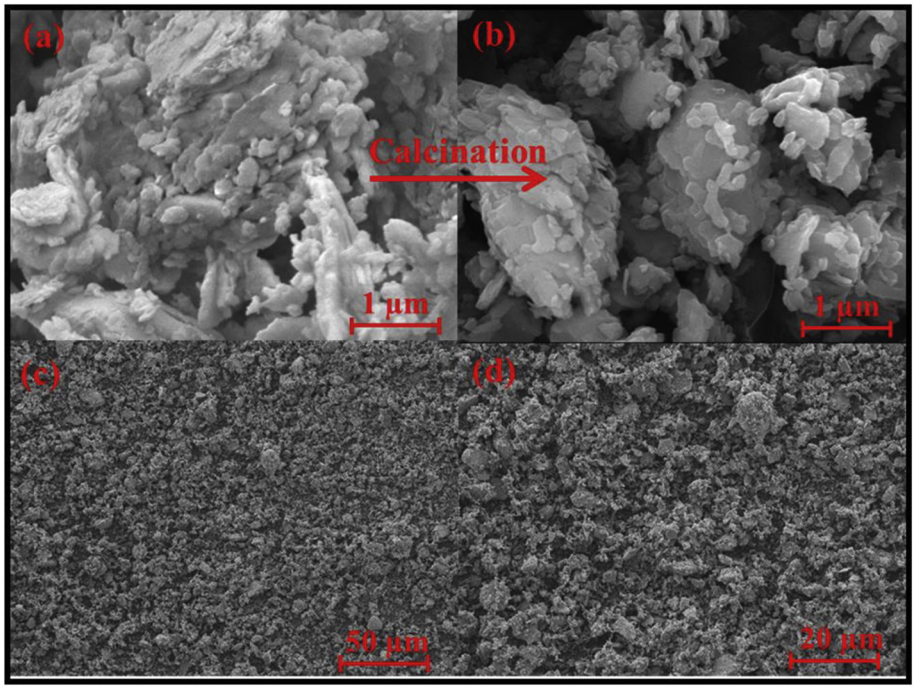

Fig. 6. Results of SEM images for kaolin: (a), (c)–(d) kaolin and (b) kaolin (T).

Table 3
Surface characteristics of three Si-Al sorbents.

Samples	Floating beads	Kaolin	Kaolin (T)
BET specific surface area (m^2/g)	3.21	4.04	4.53
Single point adsorption total pore volume of pores (cm^3/kg)	7.19	10.51	14.57
t-Point micropore volume (cm^3/kg)	0.90	1.17	0.67
Adsorption average pore width (4 V/A by BET, nm)	9.69	12.76	14.80

chemical properties. Fig. 6(c) and (d) illustrate the surface characteristics of kaolin under different resolution ratios. It can be found that the kaolin is all clumped together and the total external surface area is smaller due to a larger density. Therefore, the mineral vapors such as alkali metals are not easy to diffuse to the pores among kaolin particles, which will decrease the adsorption process.

Fig. 7(a) and (b) shows the surface characteristics of floating beads under different resolution ratios. As shown in Table 3, the irregular external surface and internal pores of floating beads improve its specific surface area and adsorption average pore width. This promotes the reaction between the silicon aluminum oxides and the alkali metals on the external and internal surface of floating beads, thereby increasing the adsorption of ultrafine particles. In addition, the shape of floating beads after high-temperature calcination is more regular and the voidage among the particles is larger than that of kaolin, which will promote the diffusion of mineral vapors to the adsorption surface. In order to verify the adsorption effect of alkali metals on the surface of floating beads, floating beads (wt. 90%) and NaCl (wt. 10%) are calcined in a muffle at 1273 K. Fig. 7(c) and (d) shows the external surface morphology of after reaction between floating beads and NaCl. It can be seen that the external surface of floating beads becomes rough due to the formation of Na-Al-Si (T). The apparent density of the floating beads, kaolin (T), and kaolin as 701 kg/m^3, 1176 kg/m^3, and 1318 kg/m^3, corresponding to the external surface area of each sorbent as 0.142 m^2/g, 0.085 m^2/g, and 0.076 m^2/g, respectively. As shown in Table 3, this indicates the internal surface area of sorbents is much larger than the external surface area, and the chemical adsorption of mineral vapors such as alkali metals mainly occurs on the internal surface. However, although the chemical adsorption on the external surface is secondary, the Na-Al-Si (T) produced by the external surface reaction, can form a molten softening layer on the external surface of the sorbents. As shown in Fig. 7(c), the cohesiveness among fine PM is enhanced due to the formation of softening layer which will lead to promote the fine PM to condense into coarse PM. Due to the external surface area of floating beads is larger than that of kaolin, the physical collision is more likely to occur on the external surface. This will be conducive to the physical adsorption of $PM_{0.5+}$ on the external surface of floating beads. This conclusion is consistent of that of Figs. 3 and 4.

As shown in Table 2, the content of SiO_2 increases slightly from 51.84% to 53.75%, and Al_2O_3 decreases from 45.73% to 43.81% after high-temperature calcination, resulting in a slight increase in the Si content in kaolin (T). As shown in Fig. 8(a), floating beads and kaolin mainly consist of mullite ($3Al_2O_3{\cdot}2SiO_2$), quartz (SiO_2) and corundum (Al_2O_3) by XRD analysis. Fig. 8(a) also presents the various band positions for the main crystalline phases in the three sorbents. For example, the mullite bands are mainly characterized by peaks at 16.7°, 21.7°, 31.0°, 40.9°, and 60.7°; the quartz bands are found in peaks at 26.2°, 53.8°, and 74.7°; and the corundum bands show peaks at 35.1°, 42.5°, and 57.6°. The different bands of each crystalline phase indicate that the crystal structure planes of the three sorbents are diverse. In addition, there is no significant difference between raw kaolin and kaolin (T) in the XRD patterns, indicating that the calcination process does not notably change the crystal structure of kaolin. However, the calcination treatment significantly increases its pore characteristics through dihydroxylation. The peak intensity of the floating beads at 26.2° is much higher than that of kaolin, indicating that the floating beads contain a higher content of SiO_2. In Table 2, it can be also found that the main components of floating beads and kaolin are SiO_2 and Al_2O_3, which account for more than 95% of the total components and the relative content of SiO_2 in the floating beads is higher than that of kaolin. This indicates that the results gained form XRF are consistent with that of XRD. Therefore, although a small part of crystallized structures are reflected in Fig. 8, the relative content of SiO_2 can be still revealed by XRD results. Many studies have shown that SiO_2 can efficiently capture alkali metal vapor; therefore, the floating beads have a

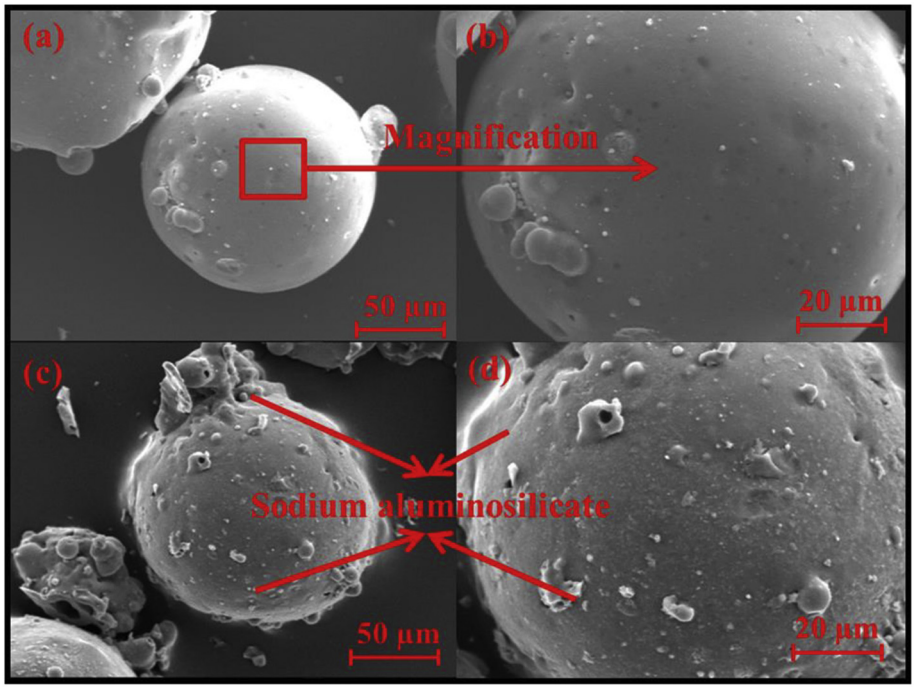

Fig. 7. Results of SEM images for floating beads: (a)–(b) floating beads, and (c)–(d) floating beads + NaCl.

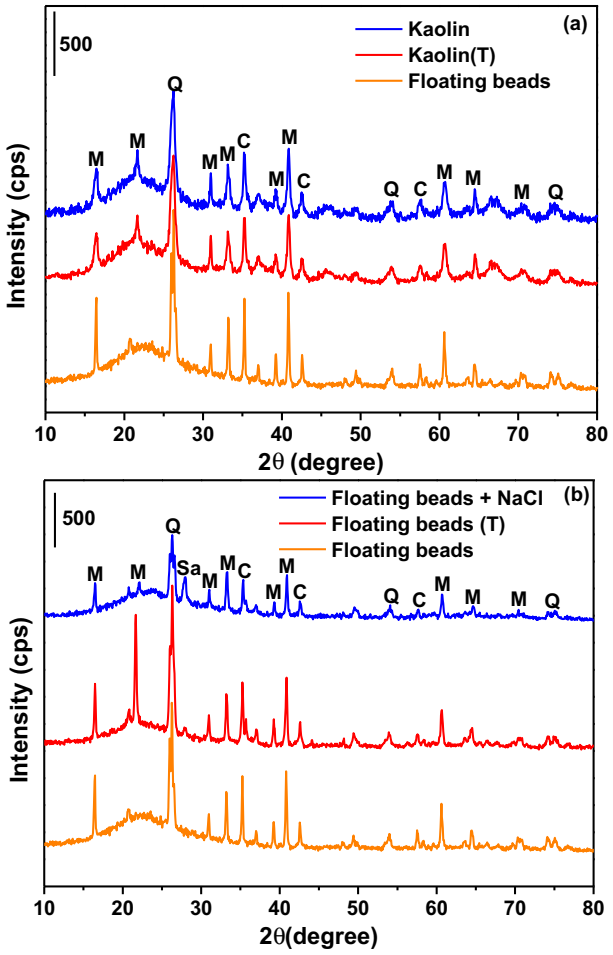

Fig. 8. XRD patterns of: (a) floating beads, kaolin, and kaolin (T); (b) floating beads, floating beads (T), and floating beads + NaCl, and the main crystalline phase can be shown as M (mullite)-$3Al_2O_3{\cdot}2SiO_2$, Q (quartz)-SiO_2, C (corundum)-Al_2O_3 and Sa (sodium aluminosilicate).

better adsorption effect on the reduction of ultrafine particles, as shown in Figs. 3 and 4.

As shown in Fig. 8(b), after high-temperature calcination, the mullite band characterized by peaks at 21.7° becomes obvious, indicating that except for quartz, mullite also plays an important role in reducing ultrafine mode particles. After the reaction between floating beads and NaCl, the mullite, quartz, and corundum bands are significantly weakened and the sodium aluminosilicate band characterized by peaks at 28.0° is enhanced. This process is mainly determined by the following reactions as:

$$SiO_2\,(s) + 2NaCl\,(s,g) + H_2O\,(g) = Na_2SiO_3\,(s) + 2HCl\,(g) \quad (R1)$$

$$Al_2O_3\,(s) + 2NaCl\,(s,g) + H_2O\,(g) = 2NaAlO_2\,(s) + 2HCl\,(g) \quad (R2)$$

$$4SiO_2\,(s) + Al_2O_3\,(s) + 2NaCl\,(s,g) + H_2O\,(g) = 2NaAlSi_2O_6\,(s) + 2HCl\,(g) \quad (R3)$$

To further clarify the reasons for the better adsorption effect of floating beads on PM reduction, the chemical bond differences among kaolin, kaolin (T), and floating beads are characterized by the FTIR. As shown in Fig. 9(a), the peaks of the Si—O—Si and Al—O—Si bands at 465 and 569 cm^{-1} are decreased after modifying the kaolin through high-temperature calcination. In addition, the Al-OH bands at 837 and 895 cm^{-1} are significantly reduced due to hydroxyl loss. Most importantly, the Si—O bands at 1095 cm^{-1} are greatly decreased after calcination, indicating that some Si—O bands break up and that more free silicon dioxide and active sites are produced in the kaolin (T). Based on the above experimental analysis and discussion, kaolin (T) mainly reduces PM emissions through two mechanisms. First, the high-temperature modification process improves the surface and pore properties of kaolin (T) and thereby promotes the surface reaction of SiO_2 and Al_2O_3 in kaolin and alkali metal vapors in the flue gas. Second, the calcination process partly destroys the internal structure of kaolin, facilitating the formation of the active free silicon dioxide and active sites, which have a higher ability to capture alkali metal vapors, thereby decreasing the ultrafine mode particle ($PM_{0.5}$) emissions. In addition to inhibiting the agglomeration of fine particles to coarse particles with the addition of sorbents, the resulting silicates and

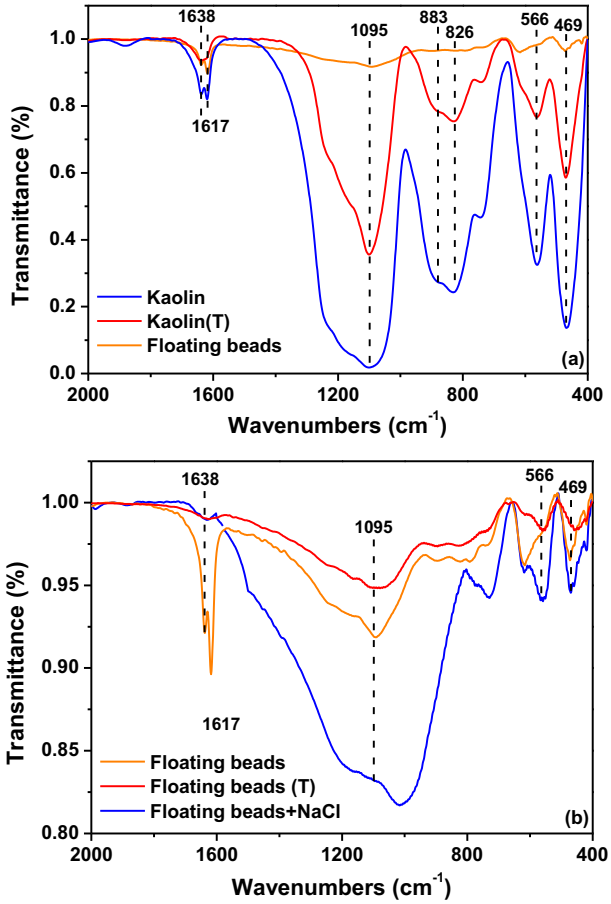

Fig. 9. FTIR spectra for: (a) floating beads, kaolin, and kaolin (T); (b) floating beads, floating beads (T) and floating beads + NaCl; the absorption bands at 469 cm^{-1} represent Si—O—Si, bands at 566 cm^{-1} represent Al—O—Si stretching vibration, bands at 826 and 883 cm^{-1} represent Al—OH, bands at 1095 cm^{-1} represent Si—O, and bands at 1617 and 1638 cm^{-1} represent —OH banding of water.

aluminosilicates can form a softening layer on the surface of sorbents to promote central mode particle ($PM_{0.5–7}$) adsorption.

As shown in Table 2, compared with kaolin, although the floating beads contain higher silica dioxide contents, the formation process makes the Si—O, Si—O—Si, and Al—O—Si bands much lower than those of kaolin and kaolin (T), indicating that the floating beads may contain more active free silicon dioxide and active sites [21], which will greatly promote the adsorption efficiency of mineral vapors such as alkali metals. This result also explains that, although the specific surface area of the floating beads is lower than that of kaolin, the PM adsorption efficiency is higher than that of kaolin due to the presence of more active free silicon dioxide. Fig. 9(b) indicates that the Si—O bands of floating beads at 1095 cm^{-1} are further decreased after calcination. However, after the reaction with NaCl, the transmittance of bands is enhanced, indicating new Si—O bands at 1095 cm^{-1}, Al-O-Si bands at 566 cm^{-1}, and Si—O—Si bands at 469 cm^{-1} are regenerated due to the formation of new components such as sodium aluminosilicate. This shows once again that the silica-aluminum oxides in the floating beads have an efficient adsorption effect on alkali metals and can significantly reduce the formation of ultrafine mode particles.

4. Discussion

For both floating beads and kaolin, their basic adsorption mechanism for minerals, such as alkali metals, depends on the active sites formed by the breaking of chemical bonds between silicon (or

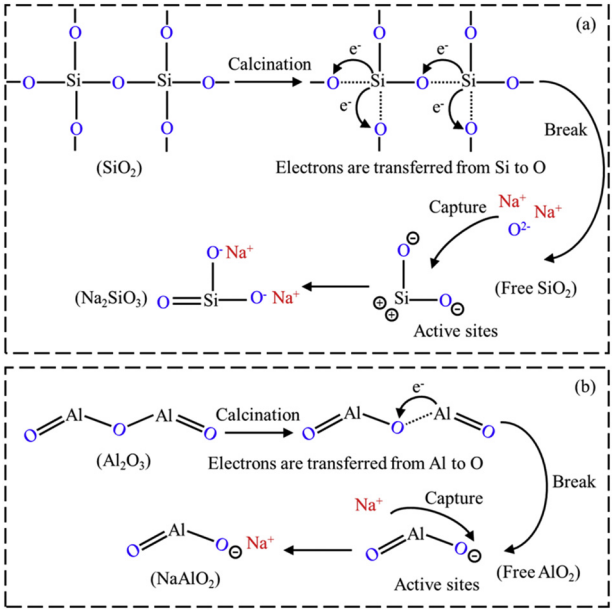

Fig. 10. The chemical adsorption of sodium by silicon and aluminum oxides.

aluminum) and oxygen, as shown in Fig. 10. The formation mechanism of active sites can be considered as the transfer of electrons from Si (or Al) to O; thus, the oxygen atoms have −1 valence in the new structural units of silica. O^- has a very strong binding force to alkali metal cations such as Na^+ and can capture large quantities of alkali metal vapors released from the coal combustion process. As shown in Fig. 10, in this paper, the relative content of active sites in floating beads and kaolin is presented by semi-quantitative of FTIR. For example, compared to kaolin, the transmittance of Si—O bonds is relatively low in floating beads, indicating that a lot of Si—O bonds are broken, which leads to the generation of more active sites. Similar reports are also mentioned in the paper by Sun et al. [10] and Zhang et al. [21]. In addition, the floating beads used in the experiments have been calcined in the furnace, so the surface characteristics of the floating beads are less affected by the combustion process.

As shown in Fig. 10(a), after high-temperature calcination, two Si—O chemical bonds break due to electron migration in the basic structural unit of silicon dioxide in floating beads and kaolin (T). At this time, Si atoms lose two electrons to form Si^{2+}, which can capture the O^{2-} in the flue gas to form new Si═O bonds. The formation of two new Si—O^- is capable of efficiently capturing Na^+ vapors to form Na_2SiO_3 due to the presence of active sites. Fig. 10(b) shows the mechanism of aluminum oxide capturing sodium vapors. Similar to silicon dioxide, calcination causes Al—O bonds in the basic structural unit of aluminum oxide to break up. Active sites can be formed through the transfer of electrons from Al to O, and the new O═Al—O^- structure can capture the alkali metal cations to form $NaAlO_2$. In fact, it is more possible to form aluminosilicates, e.g., $NaAlSi_2O_6$, under the combined action of silicon dioxide and aluminum oxide. Considering that the melting point of Na_2SiO_3 is 1362 K, that of $NaAlSi_2O_6$ is approximately 1323 K and that of $NaAlO_2$ is 1923 K, the silicates and aluminosilicates appear to easily form a softening layer on the surface of the sorbent particles, thereby promoting the adsorption of central mode particles and reducing the total amount of PM. Therefore, the floating beads have a higher content of silicon dioxide, which not only can capture a large amount of mineral vapors such as alkali metals to reduce the formation of ultrafine mode particles but also has a better control effect on the formation of central mode particles.

This above conclusion has been also confirmed by the results gained from characterization tests in Figs. 5, 8(b), and 9(b). Fig. 5 illustrates that $PM_{0.5}$ mainly consists of Na and S in the Zhundong coal

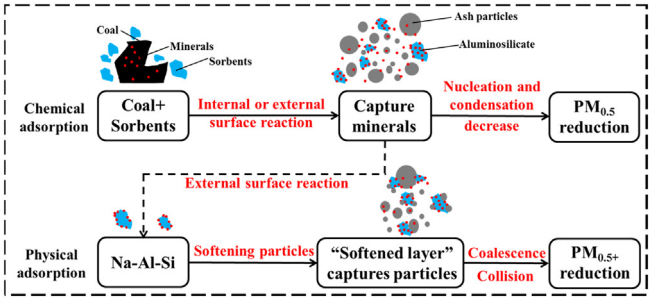

Fig. 11. Schematic diagram of PM reductions by sorbents at high temperature.

combustion used in these experiments. Therefore, because alkali metal vapors are captured in large quantities with the addition of sorbents, they reduce the chance of forming sulfate in the presence of SO_2. As shown in Fig. 4, sorbents can control the formation of ultrafine mode particles by inhibiting the homogeneous nucleation and heterogeneous condensation of Na_2SO_4. At the same time, as shown in Fig. 8(b), after high-temperature reaction of floating beads with NaCl, the peak of sodium aluminosilicate presents at 27.9°, which also confirms the reaction process shown in Fig. 10(a). This phenomenon is also been confirmed by Si et al. [8]. In addition, based on the analysis of FTIR in Fig. 9(b), the new bonds of Si—O or Al—O can be regenerated through chemical reactions due to the formation of aluminosilicate, which will lead to the increase of transmittance at the corresponding position. The reaction between Al_2O_3 and alkali metals is similar to that of SiO_2.

As stated above, the mineral vapors, e.g., alkali metals, are easily vaporized and then nucleate or condense to form ultrafine mode particles during coal combustion. Zhundong coal is used in the experiments, and the content of alkali metals and sulfur is relatively high; therefore, sulfate formation will promote $PM_{0.5}$ emissions. The char and coarse mineral fragmentation are the main sources of $PM_{0.5+}$ formation, and the main compositions are calcium, silicon, and iron. Therefore, as shown in Fig. 11, there are two pathways for PM reduction by sorbents such as floating beads. On the one hand, the ultrafine mode particle ($PM_{0.5}$) reduction is promoted by the internal and external surface reaction between minerals such as alkali metals and sorbents, thereby inhibiting the formation of sulfates by alkali metals. Therefore, the nucleation and condensation process of minerals to form $PM_{0.5}$ will be inhibited. This process steps proposed in Fig. 11 have been confirmed by our experiments in Figs. 5 and 7–9. On the other hand, due to aluminosilicate formation on the external surface of sorbents, the particles collide and coalesce with Na-Al-Si (T), which promotes the fine particles to form coarse particles and then reduces the central mode particle ($PM_{0.5-7}$) emissions. This conclusion can be confirmed by the results in Fig. 7(c) and (d). Similar results have been also found by Si et al. [8] and Zhang et al. [21], who showed that the impact factor of coalescence resulting from mineral melting was greater than that of particle collisions when studying the reduction of central mode particles. Therefore, the formation of aluminosilicates with low melting points is very important for central mode particle reduction. In addition, according to the analysis on Section 3.4, the internal surface reaction is more important for $PM_{0.5}$ adsorption than the external surface reaction due to larger internal surface area. Based on the Knudsen pore diffusion equation and adsorption average pore width (10 nm) provided by Table 3, the diffusion coefficient can be calculated as 7.14×10^{-2} cm^2/s. If the pore depth is considered to be equal to the radius (30 μm) of the sorbents, the length-time of internal diffusion can be calculated as microsecond level, indicating that the chemical adsorption time on the internal surface is sufficient to reduce $PM_{0.5}$ formation. Although the external surface reaction is secondary, the softened layer formed by Na-Al-Si (T) on the external surface is conducive to the physical adsorption of $PM_{0.5+}$ (coalescence and collision). In practical boilers, the combustion characteristics are more complicated than those in the DTFs, and the higher combustion temperature and more intense flue gas turbulence can further improve mineral melting and promote particle collision. This result indicates that floating beads (or kaolin) may exhibit a better effect on ultrafine and central mode particle control during the practical combustion of a coal-fired boiler.

5. Conclusions

In this paper, the emission characteristics of PM during combustion experiments of Zhundong coal mixed with sorbents are carried out in a lab-scale DTF. The kaolin and kaolin (T) are used as a reference to revel the PM (ultrafine and central mode) adsorption characteristics of floating beads under an O_2/N_2 atmosphere. The main conclusions are as follows:

(1) During Zhundong coal combustion, mineral vapors such as alkali metals and sulfur are the main precursors that form ultrafine particles ($PM_{0.5}$), and the yield is controlled by the homogeneous nucleation and heterogeneous condensation of mineral vapors. The central and coarse mode particles are mainly contributed by char and coarse mineral fragmentation, and the main compositions consist of Ca, Si, and Fe.
(2) Floating beads can efficiently reduce the PM emissions, and the yields of ultrafine mode particles ($PM_{0.5}$) and central mode particles ($PM_{0.5-7}$) decrease by 55.76% and 21.7%, respectively, with the addition of floating beads. Floating beads can directly capture alkali metal vapors to inhibit sulfate formation via chemisorption and thereby reduce the chance of nucleation and condensation of mineral vapors to form ultrafine mode particles. Due to aluminosilicate formation, the particles collide and coalesce with Na-Al-Si (T) via physisorption, which causes the fine particles to form coarse particles and then reduces the yield of central mode particles.
(3) Due to the broken Si—O and Al—O bonds after high-temperature calcination, floating beads and kaolin (T) produce more active free silicon dioxide and active sites and can greatly promote the adsorption efficiency of mineral vapors such as alkali metals. Compared to raw kaolin, the ability to capture ultrafine and central mode particles has been obviously improved.

CRediT authorship contribution statement

Jing Zhao: Investigation, Data curation, Methodology, Writing - original draft. **Yufeng Zhang:** Data curation, Visualization, Software. **Xiaolin Wei:** Conceptualization, Supervision, Validation, Writing - review & editing. **Teng Li:** Conceptualization, Methodology, Supervision. **Yu Qiao:** Supervision, Validation.

Declaration of competing interest

The authors declare that they have no known competing financial interests or personal relationships that could have appeared to influence the work reported in this paper.

Acknowledgments

This work is supported by the National Natural Science Foundation of China (no. 51736010). The authors also thank Prof. Minghou Xu and Prof. Dunxi Yu (State Key Laboratory of Coal Combustion, Huazhong University of Science and Technology) for supplying experimental site and facilities.

References

[1] J.B. Zhou, X.G. Zhuang, A. Alastuey, X. Querol, J.H. Li, Geochemistry and mineralogy of coal in the recently explored Zhundong large coal field in the Junggar basin, Xinjiang province, China, Int. J. Coal Geol. 82 (2010) 51–67.

[2] Y.M. Yang, Y.X. Wu, H. Zhang, M. Zhang, Q. Liu, H.R. Yang, J.F. Lu, Improved sequential extraction method for determination of alkali and alkaline earth metals in Zhundong coals, Fuel 181 (2016) 951–957.
[3] H.J. Ge, L.H. Shen, H.M. Gu, S.X. Jiang, Combustion performance and sodium absorption of ZhunDong coal in a CLC process with hematite oxygen carrier, Appl. Therm. Eng. 94 (2016) 40–49.
[4] X.B. Qi, G.L. Song, W.J. Song, S.B. Yang, Q.G. Lu, Combustion performance and slagging characteristics during co-combustion of Zhundong coal and sludge, J. Energy Inst. 91 (2018) 397–410.
[5] X.B. Wang, Z.X. Xu, B. Wei, L. Zhang, H.Z. Tan, T. Yang, H. Mikulčić, N. Duić, The ash deposition mechanism in boilers burning Zhundong coal with high contents of sodium and calcium: a study from ash evaporating to condensing, Appl. Therm. Eng. 80 (2015) 150–159.
[6] P. Glarborg, Hidden interactions-trace species governing combustion and emissions, Proc. Combust. Inst. 31 (2007) 77–98.
[7] B.Q. Dai, F. Low, A. De Girolamo, X.J. Wu, L. Zhang, Characteristics of ash deposits in a pulverized lignite coal-fired oiler and the mass flow of major ash-forming inorganic elements, Energy Fuel 27 (2013) 6198–6211.
[8] J.P. Si, X.W. Liu, M.H. Xu, L. Sheng, Z.J. Zhou, C. Wang, Y. Zhang, Y.C. Seo, Effect of kaolin additive on $PM_{2.5}$ reduction during pulverized coal combustion: importance of sodium and its occurrence in coal, Appl. Energ 114 (2014) 434–444.
[9] W.P. Linak, C.A. Miller, W.S. Seames, J.O.L. Wendt, T. Ishinomori, Y. Endo, S. Miyamae, On trimodal particle size distributions in fly ash from pulverized-coal combustion, P. Combust. Inst. 29 (2002) 441–447.
[10] W. Sun, X.W. Liu, Y.S. Xu, Y. Zhang, D. Chen, Z.G. Chen, M.H. Xu, Effects of the modified kaolin sorbents on the reduction of ultrafine particulate matter ($PM_{0.2}$) emissions during pulverized coal combustion, Fuel 215 (2018) 153–160.
[11] Z.F. Hu, X.B. Wang, A. Adeosun, R.H. Ruan, H.Z. Tan, Aggravated fine particulate matter emissions form heating-upgraded biomass and biochar combustion: the effect of pretreatment temperature, Fuel Process. Technol. 171 (2018) 1–9.
[12] G.D. Li, S.Q. Li, Q. Huang, Q. Yao, Fine particulate formation and ash deposition during pulverized coal combustion of high-sodium lignite in a down-fired furnace, Fuel 143 (2015) 430–437.
[13] M.H. Xu, D.X. Yu, H. Yao, X.W. Liu, Y. Qiao, Coal combustion-generated aerosols: formation and properties, P. Combust. Inst. 33 (2011) 1681–1697.
[14] Y. Ninomiya, L. Zhang, A. Sato, Z.B. Dong, Influence of coal particle size on particulate matter emission and its chemical species produced during coal combustion, Fuel Process. Technol. 85 (2004) 1065–1088.
[15] T. Moreno, P. Trechera, X. Querol, R. Lah, D. Johnson, Trace element fractionation between PM10 and PM2.5 in coal mine dust: implications for occupational respiratory health, Int. J. Coal Geol. 203 (2019) 52–59.
[16] Q. Yao, S.Q. Li, H.W. Xu, J.K. Zhuo, Q. Song, Reprint of: studies on formation and control of combustion particulate matter in China: a review, Energy 35 (2010) 4480–4493.
[17] K.R. Parker, Effective capture of respirable-sized particulates using electrostatic precipitator technology, Eng. Sci. Educ. J. 9 (2000) 33–40.
[18] J. Chen, H. Yao, P.A. Zhang, L. Xiao, G.Q. Luo, M.H. Xu, Control of PM_1 by kaolin or limestone during O_2/CO_2 pulverized coal combustion, P. Combust. Inst. 33 (2011) 2837–2843.
[19] J.J. Helble, Model for the air emissions of trace metallic elements from coal combustors equipped with electrostatic precipitators, Fuel Process. Technol. 63 (2000) 125–147.
[20] Y.S. Xu, X.W. Liu, Y. Zhang, W. Sun, Y.C. Hu, M.H. Xu, A novel Ti-based sorbent for reducing ultrafine particulate matter formation during coal combustion, Fuel 193 (2017) 72–80.
[21] Y. Zhang, X.W. Liu, Y.S. Xu, W. Sun, M.H. Xu, Investigation of reducing ultrafine particulate matter formation by adding modified montmorillonite during coal combustion, Fuel Process. Technol. 158 (2017) 264–271.
[22] J. Chen, F. Jiao, Z.B. Dong, O. Niyomura, T. Namioka, N. Yamada, Y. Ninomiya, Effect of kaolin on ash partitioning during combustion of a low-rank coal in O_2/CO_2 atmosphere, Fuel 222 (2018) 538–543.
[23] K.Q. Tran, K. Iisa, B.M. Steenari, O. Lindqvist, A kinetic study of gaseous alkali capture by kaolin in the fixed bed reactor equipped with an alkali detector, Fuel 84 (2005) 169–175.
[24] X.J. Chen, S.B. Liaw, H.W. Wu, Important role of volatile-char interactions in enhancing PM1 emission during the combustion of volatiles form biosolid, Combust. Flame 182 (2017) 90–101.
[25] T. Takuwa, I. Naruse, Detailed kinetic and control of alkali metal compounds during coal combustion, Fuel Process. Technol. 88 (2007) 1029–1034.
[26] L. Zhang, Y. Ninomiya, Q.Y. Wang, T. Yamashita, Influence of woody biomass (cedarchip) addition on the emissions of PM_{10} from pulverised coal combustion, Fuel 90 (2011) 77–86.
[27] Y. Ninomiya, Q.Y. Wang, S.Y. Xu, K. Mizuno, I. Awaya, Effect of additives on the reduction of $PM_{2.5}$ emissions during pulverized coal combustion, Energy Fuel 23 (2009) 3412–3417.
[28] Q.Y. Wang, L. Zhang, A. Sato, Y. Ninomiya, T. Yamashita, Effects of coal blending on the reduction of PM_{10} during high-temperature combustion 1. Mineral transformations, Fuel 87 (2008) 2997–3005.
[29] H. Li, D.L. Xu, S.H. Feng, B.M. Shang, Microstructure and performance of fly ash micro-beads in cementitious material system, Constr. Build. Mater. 52 (2014) 422–427.
[30] P.J. Van Eyk, P.J. Ashman, Z.T. Alwahabi, G.J. Nathan, The release of water-bound and organic sodium from Loy Yang coal during the combustion of single particles in a flat flame, Combust. Flame 158 (2011) 1181–1192.
[31] B.J.P. Buhre, J.T. Hinkley, R.P. Gupta, P.F. Nelson, T.F. Wall, Fine ash formation during combustion of pulverised coal-coal property impacts, Fuel 85 (2006) 185–193.
[32] X.P. Gao, Y. Li, M. Garcia-Perez, H.W. Wu, Roles of inherent fine included mineral particles in the emission of PM_{10} during pulverized coal combustion, Energy Fuel 26 (2012) 6783–6791.
[33] R.J. Lang, Anion effects in alkali-catalysed steam gasification, Fuel 65 (1986) 1324–1329.
[34] T.F. Wall, R.A. Greelman, S.K. Gupta, C. Coin, A. Lowe, Coal ash fusion temperatures—new characterization techniques, and implications for slagging and fouling, Prog. Energ. Combust. Sci. 24 (4) (1998) 345–353.
[35] H. Yao, I. Naruse, Combustion characteristics of dried sewage sludge and control of trace-metal emission, Energy Fuel 19 (2005) 2298–2303.